Biochemistry Letters, 19(1) 2023, pages 78-102

Scientific Research & Studies Center-Faculty of Science- Zagazig University- Egypt

Biochemistry Letters

Journal home page:

Oligomeric proanthocyanidin grape seed extracts inhibited oncogenic signaling crosstalk of ERK1/2, β-catenin, and STAT3 through apoptosis induction in human liver and breast cancer cell lines.

Rana H. Alneanaey[1], Nabil M. Taha[1], Mohamed A. Lebda[1], Aml E. Hashem[1], Ahmed S. Sultan[2, 3]

[1]Department of Biochemistry, Faculty of Veterinary Medicine, Alexandria University, Alexandria, Egypt. [2]Department of Biochemistry, Faculty of Science, Alexandria University, Alexandria, Egypt. [3]Department of Oncology, Lombardi Comprehensive Cancer Center, Georgetown University Medical Center, Washington DC. USA.

Corresponding Author:

Prof. Dr. Ahmed S. Sultan,

Biochemistry Department, Faculty of Science, Alexandria University, Alexandria, Egypt & Department of Oncology, Lombardi Comprehensive Cancer Center, Georgetown University Medical Center, Washington DC. USA. Tel: +201222267463 Egypt, +1202-600-6560. E-mail: dr_asultan@alexu.edu.eg & As4048@georgetown.edu. https://orcid.org/0000-0001-9 6568-1757.

First Author:

Rana H. Alneanaey,

Ph.D. candidate at Biochemistry Department, Faculty of Veterinary Medicine, Alexandria University, Egypt.

E-mail: rana.ateya.vet8@alexu.edu.eg. https://orcid.org/0000-0002-0727-9804

Second Author:

Prof. Dr. Nabil M. Taha,

Professor of Biochemistry. Faculty of Veterinary Medicine -Alexandria University, Egypt. E-mail: prof_nabil2006@yahoo.com

Third Author:

Prof. Dr. Mohamed A. Lebda,

Professor of Biochemistry. Chairman of Biochemistry Department. Faculty of Veterinary Medicine -Alexandria University, Egypt. E-mail: Lebdam1979@alexu.edu.eg. https://orcid.org/0000-0003-2548-5465.

Fourth Author:

Dr. Aml E. Hashem,

Assistant professor of Biochemistry. Faculty of Veterinary Medicine -Alexandria University, Egypt. E-mail: Amlhashem@alexu.edu.eg. https://orcid.org/0000-0001-9941-4163.

.

Biochemistry letters, 19 (1) 2023, Pages 78-102

ARTICLE INFO
Received : 29/8/2023
Accepted : 7/9/2023
Available online : 16/9/2023

Keywords:
OPC-PACs; p-ERK, ZR-75 1, STAT-3, β-catenin, Grap seeds.

ABSTRACT

Background: The constitutively activated oncogenic signals of ERK, β-catenin, and signal transducer and activator of transcription-3 (STAT-3) are therapeutic targets in cancer treatment. The present study explored the anticancer mechanism of grape seed extract's polyphenolic compounds, Oligomeric-Proanthocyanidins (OPC-PACs), to combat oncogenic proliferative signaling crosstalk, as the precise mechanisms are not yet fully understood. **Materials and Methods:** The mechanistic anti-cancer effects of the OPC-PACs on oncogenic signaling crosstalk and apoptosis-induction were investigated, using liver and breast cancer cell lines (HepG2 and ZR-75-1), *in vitro* and by measuring tumor volume of MNU-induced mammary tumors, *in vivo*. **Results:** Wst-1 assay demonstrated that the viability of OPC-PACs treated cells was significantly decreased in a concentration-dependent manner compared to the mock. The calculated IC_{50} was (63.1 ± 0.024 mg/ml) and (61.6 ± 0.016 mg/ml) for HepG2 and ZR-75-1, respectively. Furthermore, OPC-PAC treatment for 48 h induced cell morphological changes, histone release, increased caspase-3 activity, and inhibition of p-ERK, β-catenin, and STAT-3 expression with apoptosis induction in HepG2 and ZR-75-1 cell lines as well as inhibition of tumor volume *in vivo*. *In vivo*, OPC-PAC treatment for 45 days significantly ($p < 0.05$) decreased the tumor size of MNU-induced mammary tumors by 28.7% compared to untreated-induced tumors. *In-vivo* cytotoxicity assessment confirmed the safety of the OPC-PACs treatment. **Conclusion:** The present study introduces OPC-PAC extract as a natural, non-toxic, and significantly inhibited crosstalk involved in cell proliferation that might act as a promising protective compound for consideration in complementary therapy in human cancers.

.

1. Introduction:

Cancer is a genetic disease caused by genetic changes that control the cells' function, especially how they grow and divide. In 2020, it was recorded that the leading cause of death among several diseases globally is cancer, and approximately 10 million deaths have been reported because of cancer in the same year (1).

Polyphenolic compounds have two main classes, flavonoids, and non-flavonoids, which have a significant health benefit (2). Some flavonoids, including flavan-3-ols catechin and epicatechin, are polymerized to produce tannins with characteristics like hydrolysis and condensation and are considered secondary plant metabolites (3). Condensed tannins, called Proanthocyanidins (PAC), consist of the oligomers or polymers of flavan-3-ol molecules linked together through interfluve linkages (4). PACs are classified into monomers, oligomers, and polymeric proanthocyanidins (4). The primary biological activity of oligomers extract

is much higher than the polymeric extract, so it is vital to degrade polymeric contents to get the oligomer's portion.

Recently, attention has been raised to finding naturally nontoxic anticancer agents from naturally occurring products. Many fruits are widely consumed and have significant health benefits, and one of them is Grapes, which contain 60% to 70% of PACs in their seeds (5,6). Extracts from natural plants have prevented and treated numerous clinical diseases, including cancer. Among these natural products are oligomeric Proanthocyanidins (OPC-PACs), considered the most significant component of grape seeds and have an anti-inflammatory and antioxidant *in vitro* (7,8). The primary class of polyphenols is OPC-PACs, which are widespread in fruits, nuts, cocoa-based products, berries, beans, and beer (9). Furthermore, OPC-PACs have anti-cancer effects by modulating several gene expressions that influence cancer prognosis (10). In addition, several NF-κB-responsive genes such as COX-2 (inducible nitric oxide synthase) proliferating cell nuclear antigen, cyclin D1, and MAPK proteins are suppressed by the action of OPC-PACs (11), leading to modulating cellular growth, proliferation, and induce apoptotic effects which in turn introducing OPC-PACs as effective modulators in treating and preventing of many cancers (10,12).

Many liquid/liquid-based methods are applied to extract PACs, such as methanol, ethanol, or acetone, using some aqueous organic solutions as an extraction solvent (13). For more efficient extraction of the PACs, ATPE (aqueous two-phase extraction) methods use salt solutions as ionic liquids (13,14). The most preferred efficient solvent for the extraction of the bioactive pants is ethanol because of its minimal toxicity and adequate extraction capacity (15). In addition, the extraction of OPC-PACs using aqueous/ethanol-based methods is preferred and favorable for medical, food, and nutraceutical applications.

Several key-signaling pathways are essential for the progression of several cancers, such as Wnt/β-catenin, Mitogen-activated protein kinase (MAPK), and Signal transducer and activator of transcription-3 (STAT-3). Firstly, Wnt/β-catenin is responsible for forming adherens junctions to produce a stable complex in the presence of cell adhesion proteins of the cadherin family (16). However, in the free nonphosphorylated state, Wnt/β-catenin signaling is responsible for the accumulation of β-catenin in the cytoplasm and then translocated into the nucleus to control the expression of target genes that are responsible for cellular proliferation, differentiation, and metastasis through the interaction with the T-cell factor transcription factors, indicating that Wnt/β-catenin has a vital role in the proliferation and cancer progression in different organs (17,18).

Secondly, MAPK significantly controls cellular proliferation, differentiation, and apoptosis (19). Activation of the MAPK/ERK signaling pathway promotes the growth of liver and breast cancer(20). On the contrary, blocking of MAPK/ ERK signaling pathway regulates the proliferation of human liver and breast cancers, indicating that MAPKs are responsible for cancer initiation and metastasis(21). In addition, the activated MAPK/ERK axis plays a vital role in the advanced progression of HCC (22).

Lastly, STAT-3 activation is started by binding growth factors, cytokines, and several peptide ligands, followed by tyrosine phosphorylation

in the cytoplasm, which leads to phosphorylation and activation of STAT-3. After activation, the STAT-3 dimers translocate into the nucleus, where the STAT-3 dimers bind to specific target genes and act as a transcription factor to regulate and control cellular proliferation, apoptosis, and differentiation (23).

The present study was performed to provide important unrecognized insights into the molecular mechanisms underlying anticancer activities exerted by oligomeric Proanthocyanidins (OPC-PACs) extracted from grape seeds by aqueous ethanol-based method in vitro and in vivo. All in all, we shed light on the crosstalk among three oncogenic signaling pathways such as p-ERK, STAT-3, and Wnt/β-catenin that play a role in cancer progression and provide a rationale for their use as a potential source of molecular target-based cancer prevention.

2. Materials and methods:

2.1 Materials:

Three bunches of red and green grapes were purchased from the local market in Alexandria, Egypt. Aqueous ethanol (P016EAAN) used for Oligomeric Proanthocyanidins (OPC-PACs) extraction was provided by Commercial Alcohols, Brampton, ON, Canada. Procyanidin B2 (42157) was obtained from MilliporeSigma, Oakville, ON, Canada. Oligomeric Proanthocyanidins (OPC-PACs) from grape seeds (1298219) were obtained from USP, Rockville, MD, USA, to be used as a standard for HPLC analysis.

Dulbecco`s Modified Eagle`s Medium, with 4,5 g/l Glucose, with LGlutamine (DMEM), was obtained from (Lonza Biowhittaker, Brazillian Origin) supplemented with 10% Fetal bovine serum (FSB) from (Lonza Biowhittaker, Brazillian Origin) and 1% of Penicillin /streptomycin 10:000 U Penicillin/ml 10:000U Streptomycin/ml from (Lonza Biowhittaker, Brazillian Origin). Cell proliferation reagent WST-1 was obtained from (Abcam, Cambridge, MA, USA). Phosphate-buffered saline (PBS) and 10% buffered formalin were obtained from (Lonza Biowhittaker, Brazillian Origin). BCA assay was obtained from (Thermo Fisher Scientific Inc., Pierce Biotechnology, Rockford, USA). Ultra-Cruz™ Nitrocellulose pure transfer membrane was obtained from (Santa Cruz Biotechnology, Santa Cruz, CA, USA). Ultra TMB (3,3',5,5'tetramethylbenzidine) was purchased from (Sigma-Aldrich, California, USA). β- catenin, Total ERK, Phosphorylated ERK, STAT3, and BAX antibodies were obtained from (Santa Cruz Biotechnology, CA, USA). Absolute methanol was obtained from (Sigma Aldrich UN). 2% crystal violet was obtained from (Oxford Laboratory Reagent). Quantity one Bio-Rad software was obtained from (Bio-Rad Laboratories, USA). Caspase three colorimetric assay was obtained from Sigma Aldrich, Saint Louis, Missouri 63103, USA.

2.2 Cell lines and culture:

HepG2 liver cancer cell line HB-8065^{TM} and Zr-75-1 breast cancer cell line CRL-1500™ were purchased from American Type Culture Collection (ATCC, Manassas, VA, USA) and cultured at 37 °C in a humidified atmosphere of 5% CO_2. HepG2 and Zr-75-1cells were cultured in Dulbecco`s Modified Eagle`s Medium, with 4,5 g/l Glucose, with L-Glutamine (DMEM). All media were supplemented with 10% Fetal bovine serum (FSB) and 1% Penicillin /streptomycin 10:000 U Penicillin/ml 10:000UStreptomycin/ml (24).

2.3 Extraction of OPC-PACs from grape seed by aqueous Ethanol:

Grape seeds were carefully selected without damage and were de-stemmed, crushed, and pressed. The juice and skin were discarded, and the grapes' origins were separated for further analysis. Extracts were prepared from powdered grape seed by diluting 150 g of powdered grape seed in 300 ml of Aqueous Ethanol (ethanol/water) solution (50:50 v/v) at 40°C for 15 minutes and by using magnetic stirring in the dark for 30 min and then centrifuged for 10 min at 4000 rpm. The supernatant was diluted with the extraction solvent (50 ml total volume). After centrifugation for 10 minutes, solids were separated at 4000 rpm, and the extraction was repeated following the same procedure. The aqueous concentrates were freeze-dried by evaporating the combined supernatant under a vacuum, ethanol was removed, and to get powdered extracts of grape seed (25).

2.4 HPLC analysis of OPC-PACs extracted by the aqueous Ethanol:

OPC-PACs composition extracted from grape seeds was determined by HPLC analysis, using the following standard of oligomeric OPC-PACs (50 µg/mL) and procyanidin B2 (25 µg/ml) in 80% ethanol/water. 0.22 µm filters were used to filter all the tested samples before injecting them into the HPLC. The HPLC system had an Xselect® HSS C_{18} 5 µm column (4.6 × 150 mm, Waters, Milford, MA, USA). It consisted of a Waters 2695 separation module and a Waters 2996 photodiode array (PDA) detector (Waters, Milford, MA, USA). The HPLC separation mobile phases were solvent A (0.1% formic acid in water) and solvent B (acetonitrile), with a 0.7 mL/min flow rate. HPLC sample injection volume was 10 µL, and PDA detection was set to 280 nm wavelength.

2.5 Cell viability and IC_{50} determination:

The IC_{50} of OPC-PACs was determined using Wst-1 assay. Cells were seeded at a density of 3 X 10^4 cells/well in a final 100 µl culture volume in a humidified atmosphere, 37°C, and 5 % CO_2. Then ten µl/well cell proliferation reagent WST-1 was added and mixed well. Cells were incubated for 4 hours in a humidified atmosphere, 37°C, and 5 % CO_2. The optical densities (OD) were measured at 450 using an ELISA reader.

2.6 Cell Morphology:

The morphological changes of cells were examined before and after the treatment with OPC-PACs to test the effect on the morphology of HepG2 and Zr-75-1 cell lines, respectively. Equal numbers of cells/well were seeded onto 12-well plates and treated with appropriate concentrations of OPC-PACs (¼ IC_{50}, ½ IC_{50}, IC_{50}) for 48 h. Cells were washed with Phosphate-buffered saline (PBS) and fixed with 10% buffered formalin (26). An inverted microscope with magnification 400X examined cells. Digital images were obtained with Kodak's tiny digital camera.

2.7 Cell Death Detection Enzyme-Linked Immunosorbent Apoptosis Assay (ELISA):

The tested cells were seeded at a density of (3×10^4) in a 96-well plate for 24 h and then incubated in media with or without different concentrations of OPC-PACs (1/4 IC_{50}, 1/2 $IC_{50,}$ and IC_{50}) for 48 h. ELISA reader detected histone release from fragmented DNA of apoptotic cells at 405 nm according to the manufacturer's protocol Cell Death Detection Kit (Roche-Applied Science, Indianapolis, USA).

2.8 Caspase-3 Activity:

Caspase-3 activities were determined according to the manufacturer's protocol kit (Bio Vision, Inc., CA, USA). Cells were seeded at a density of 5×10^6 and

then incubated for 48 h in media with or without different concentrations of oligomeric OPC-PACs (1/4 IC_{50}, 1/2 $IC_{50,}$ and IC_{50}) for 48 h. An ELISA reader measured optical density at 405 nm.

2.9 Clonogenic Assay:

HepG2 and Zr-75-1 cell lines were seeded at 1,000 cells per good density and reached optimal population densities within 24h. cells were treated with (¼ IC_{50}, ½ IC_{50} and IC_{50}) OPC-PACs for 48h and untreated control. After the treatment, the media containing the different treatments were removed and replaced with 2ml of fresh culture medium per well. The medium was replaced every three days. After 15 days of culture, colonies were washed with PBS twice, fixed with absolute methanol for 20 min, and stained with 2% crystal violet for 3 min. The dye was discarded, and colonies were washed with PBS several times. Digital images of the colonies were obtained using Kodak digital camera, and colonies were counted using Quantity One analysis software (Bio-Rad).

2.10 Western Blotting Assay:

Radioimmunoprecipitation assay Buffer (RIPA buffer)- The protease containing Lysis buffer for Western blotting- was added to cells, and total proteins were then extracted by high-speed centrifuge at 15,000 g/min (27,28). After quantifying its concentration with BCA assay, 50 µg protein samples were subjected to 10~12% Sodium dodecyl sulfate - Poly Acrylamide Gel Electrophoresis (SDS -PAGE) separation. Next, the gels were transferred onto UltraCruz™ Nitrocellulose pure transfer membrane and blocked with 5% BSA for one h. The membranes incubated with the following primary antibodies mouse monoclonal antibodies directed to (β-catenin, Total-ERK, Phosphorylated-ERK, STAT-3, and BAX) (1:1000) dilution. The membranes were washed thrice with TBST and incubated with the secondary anti-mouse monoclonal antibodies (1:5000) for one h. After passing by TBST three times, Ultra TMB (3,3',5,5'tetramethylbenzidine) was used to visualize the bands colorimetrically according to the manufacturer protocol (Sigma-Aldrich, USA)**.** Densitometry of bands was performed using Quantity One analysis software (Bio-Rad Laboratories, USA).

2.11 Animals

Virgin female albino Swiss mice (Mus musculus) as a mammalian model. 22−25 g weighing, 5–6 weeks old, 30 healthy animals were purchased from Medical Research Institute, Alexandria, Egypt. The animals were housed 5 per cage in controlled temperature and humidity, 12 h day and night cycle. They were fed a standard laboratory diet and had access to water ad libitum. All the mice experiments were conducted under the Institutional Animal Care and Use Committee procedures and guidelines of Alexandria University (Appendix 012, Guiding Principles for Biomedical Research Involving Animals).

2.12 Carcinogen Preparation

To prevent decomposition, MNU must be stored below 2-8°C in the dark. The stock container of MNU and vials containing the carcinogen were kept on ice. The injection vials were wrapped in aluminum foil and stored over desiccant until they were used because MNU is sensitive to light and humidity. The MNU was dissolved immediately before its use in 0.9% NaCl solution acidified to pH 4 with 0.05% acetic acid. The solubility of MNU in water at room temperature was 1.4 % (w/v).

2.13 Experimental Design

Animals were divided into three groups of 10 mice each into the following groups: Mock - healthy controls without MNU-induction, induced untreated-MNU given intraperitoneally (30 mg/kg) a dose that produces a high incidence of mammary tumors, and induced treated-MNU plus LD_{50} OPC-PACs._MNU (30 mg/kg body weight) was injected along

the ventral midline of the rat, halfway between the third and fourth pairs of mammary glands, using <21-gauge needles alternately through the left and right abdominal wall. The OPC-PACs were injected intraperitoneally (1ml/kg body weight); all control animals received an injection of the solvent, saline. Afterward, mice were treated three times a week for 45 days. Mice were weighed weekly and palpated twice a week after the third NMU injection to detect mammary tumors using a digital caliper. Palpable mammary tumors were seen within 90–120 days after injection. Sera were collected from the sacrificed mice for liver and kidney biochemical analysis to examine the possible toxicity. At the end of the treatment, the mice were sacrificed and anesthetized by CO_2 inhalation shortly, and their mammary glands were evaluated for the presence of tumors. The dissected animals with tumors were photographed to provide identification records on the lesions' location and gross morphology. Immediately after euthanasia, blood was obtained for hematological examination. All palpable tumors were excised, weighed, and their size and location were recorded. All palpable tumors of mammary glands and control mammary glands were excised and fixed in 10% buffered formalin. Tissues were then processed for routine histopathological evaluation. For the cytotoxicity examination, the sera from Wister Albino mice were obtained from the interior vena cava into plain sample tubes, allowed to stand for two h, and centrifuged to separate serum from the blood cells. Sera were analyzed spectrophotometrically for liver and kidney functions, including the activities of AST and ALT, creatinine, and total protein (29–31).

2.14 Statistical Analysis:

Data obtained as the mean ± SDM for three independent experiments were subjected to ANOVA (A one-way analysis of variance) using SPSS-IBM software, version 20 (SPSS Inc., Chicago, IL, USA). Tukey's honestly significant difference (HSD) post hoc test ($P < 0.05$) was used following ANOVA. Statistically, significance was detected by calculating P-value versus control cells; *P-value < 0.05; **$P < 0.01$ and ***$P < 0.001$ were considered statistically significant.

3. Results:

3.1 HPLC Analysis of the Extracted OPC-PACs

HPLC and the HPLC chromatogram analyzed oligomeric composition was compared with the standard of procyanidin B2 (dimeric PAC) and OPC-PACs oligomeric standard as shown in **(Figure 1).** The fraction of grape seed OPC-PACs was comprised of peaks procyanidin B2 (24-26 min), and oligomeric PAC (32–44 min).

3.2 OPC-PACs inhibit the Proliferation of $HepG_2$ and Zr-75-1 Cells.

To investigate the inhibitory effect of Oligomeric OPC-PACs on cellular viability and proliferation in HCC and human breast cancer cell lines, two different cell lines, $HepG_2$ and Zr-75-1 cells, by using WST-1 assay. $HepG_2$ and Zr-75-1 cells were treated with different concentrations ranging (from 0 ~120 mg/mL) oligomeric OPC-PACs for 48 h. As demonstrated in **(Figure 2A and 2B),** Oligomeric OPC-PACs reduced the viability of $HepG_2$ and Zr-75-1 cells in a dose-dependent manner after 48 h. OPC-PACs' IC50 was calculated to determine the appropriate treatment dose for subsequent experiments.

Treatment of HepG2 or Zr-75-1 cells with increasing concentrations of OPC-PACs resulted in a significant cell death and inhibition of cell viability in a dose-dependent manner compared to the control as determined by Wst-1 assay after 48 h **(Figure 2A and 2B).** Furthermore, the effective significant inhibitory concentrations of OPC-PACs

started at 31.55 and 30.8 mg/ml for HepG2 or Zr-75-1 cells, respectively. The concentration at which 50% inhibition of treated cell viability was achieved, $IC_{50,}$ was calculated using a semi-logarithmic plotting of the percentage of cell viability versus the concentration. The calculated IC_{50} of oligomeric OPC-PACs was (63.1 ±**0.024** mg/ml) and (61.6 **± 0.016** mg/ml) for HepG2 and Zr-75-1, respectively, as shown in **(Figure 2A and 2B).**

Cell viability and proliferation of both tested cell lines were inhibited after treatment with different concentrations of oligomeric OPC-PACs for 48 h. We focused on the mechanistic inhibitory effect of OPC-PACs on HepG2 and Zr-75-1 cells that showed a high sensitivity for oligomeric OPC-PACs after 48 h.

3.3 OPC-PACs induce morphological changes in $HepG_2$ and Zr-75-1 Cells.

To confirm the decrease in cell viability and the apoptotic induction in both $HepG_2$ and Zr-75-1 cell lines, morphological changes were determined using microscopy after treatment of both cell lines with or without (¼ IC_{50}, ½ $IC_{50,}$ and IC_{50}) oligomeric OPC-PACs for 48 h. As shown in **(Figure 3A and 3B)**, the apoptotic morphological changes showed shrinkage, rounded and detached cells, the loss of cell junction, and severe disruption from the cell culture substratum. The apoptotic cell death characteristics became visible after treatment with several doses of OPC-PACs for 48 h compared to untreated control cells. The morphological changes became more remarkable with the increased concentration of oligomeric OPC-PACs treatment, as shown in **(Figure 3A and 3B).**

3.4 Apoptotic assay, using Apoptotic Enzyme-Linked immunosorbent, ELISA.

ELISA apoptotic assay was performed to determine histone release protein from apoptotic cells, as shown in the left panel in **(Figure 4A and 4B)** to examine if the decrease in cell viability could be due to apoptosis induction. HepG2 and Zr-75-1 cells were treated with or without (¼ IC_{50}, ½ $IC_{50,}$ and IC_{50}) oligomeric OPC-PACs, and apoptotic induction was determined as indicated by histone release according to the manufacturer's protocol compared to untreated control cells. Cells treated with (¼ IC_{50}, ½ $IC_{50,}$ and IC_{50}) OPC-PACs-induced cell death as a relatively late event, starting at 48 h compared to control. The induction of apoptosis was significantly higher in HepG2 and Zr-75-1 cells compared to untreated control cells, which showed minimal apoptotic processes.

3.5 Caspase-3 Activity in both HepG2 and Zr-75-1 Cells

Activating a cascade of intracellular cysteine proteases of caspases is the main characteristic of apoptosis (32). The typical morphological and biochemical feature observed in apoptosis is the cleavage of various substrates. Caspase-3 is considered a general mediator of physiological and stress-induced apoptosis due to the diversity of its substrates (33,34). To investigate the effect of oligomeric OPC-PACs on caspase-3 activation in treated HepG2 and Zr-75-1 cells, caspase-3 activity was assayed according to the manufacturer's protocol kit (Bio Vision, Inc., CA, USA). Our data indicated that the OPC-PACs treatment showed a significant increase in caspase-3 activity in treated cells compared to control after 48 h, as shown in the right panel **(Figure 4A and 4B).** These results confirmed that OPC-PACs treatment-induced apoptosis in HepG2 and Zr-75-1 cells in a caspase-dependent manner.

3.6 Effect of OPC-PACs on clonogenicity of HepG2 and Zr-75-1 Cell lines

A clonogenic assay was performed according to the protocol described under

the materials and methods section to investigate the capability of single HepG2 or Zr-75-1 cells to grow into a large colony through clonal expansion. Assessment of the colony-forming ability of a single cell of each of HepG2 or Zr-75-1 cells was examined before and after treatment with or without oligomeric OPC-PACs for 48 h.

Our data indicated that (¼ IC_{50}, ½ $IC_{50,}$ and IC_{50}) OPC-PACs showed a significant decrease in both HepG2 and Zr-75-1 cells clonogenicity compared to untreated control cells after 48 h. As shown in **(Figure 5A and 5B)**, the more increased concentrations of the OPC-PACs treatment, the more decreased clonogenicity of treated cells. The clonogenic assay revealed that cells treated by (¼ IC_{50}, ½ $IC_{50,}$ and IC_{50}) OPC-PACs resulted in dramatic inhibition of cell clonogenicity in a dose-dependent manner compared to the control **(Figure 5A and 5B).**

3.7 Effect of OPC-PACs on signaling pathways in HepG2 and Zr-75-1 Cells using Western Blot analysis.

To evaluate the effect of oligomeric OPC-PACs on several oncogenic signaling pathways such as β-catenin, p-ERK, Bax, and STAT3 of $HepG_2$ and Zr-75-1 cell lines, western blot analysis was performed using different concentrations of OPC-PACs for 48 h. Compared with the expression levels of control cells, western blot analysis revealed that (¼ IC_{50}, ½ $IC_{50,}$ and IC_{50}) OPC-PACs treatment significantly decreased expression levels of β-catenin, p-ERK, and STAT-3 in a dose-dependent manner in both $HepG_2$ and Zr-75-1 cell lines as shown in **(Figure 6A and 6B).** The relative density of immunoreactive bands was significantly decreased with increasing OPC-PACs concentration, indicating the inhibitory effects on cell viability and apoptosis induction, as shown in **(Figure 6A and 6B).** In the HepG2 cell line, the inhibition of β-catenin expression started at ¼ IC_{50} and significantly increased at IC_{50}. Zr-75-1 cell line showed the same response to OPC-PACs treatment. Treated HepG2 cells showed a more inhibitory effect in the expression levels of β-catenin than its expression levels of the Zr-75-1 cell line after treatment with OPC-PACs for 48h. Both cell lines showed a remarkable inhibitory effect in the expression of p-ERK compared to T-ERK, and this effect started at ¼ IC_{50} OPC-PACs. and became more significant at IC_{50} OPC-PACs. In the HepG2 cell line, OPC-PACs treatment inhibited STAT-3 expression levels, and the most effective result was detected at IC_{50}. Stat3 inhibition was seen more in the case of HepG2 cells compared to Zr-75-1 cells after treatment by ¼ and ½ IC_{50} OPC-PACs for 48h, suggesting the strong inhibitory effect of OPC-PACs on several oncogenic signaling pathways in both tested cell lines.

On the other hand, OPC-PACs treatment upregulated Bax protein expression gradually in a dose-dependent manner with increasing OPC-PACs concentration. The HepG2 cell line showed a higher upregulation in Bax expression compared to the expression levels of the Zr-75-1 cells line and untreated control, indicating that this data is consistent with OPC-PACs data of increased caspase-3 expression and released histones as markers of apoptotic induction. Moreover, the calculated relative density of immunoreactive bands was significantly increased with increasing OPC-PACs concentration, as shown in **(Figure 6A and 6B).** Our results suggested that OPC-PACs inhibited cell viability and induced apoptosis in HepG2 and Zr-75-1 cells.

3.8 *In vivo*, OPC-PACs treatment significantly decreases the MNU-induced tumor size with no cytotoxicity.

As shown in **(Figure 7A)**, the first MNU-induced palpable mammary tumors first appeared four weeks after the third application of MNU in induced mice. At this time, only 6 of the 30 mice developed grossly detectable tumors. Tumor incidence increased with time, and at the end of the experiment, 30 mice had grossly palpable mammary tumors. In addition, no statistically significant differences in body weight were observed among tested groups throughout tumor development (data not shown). The treated mice group was given LD_{50} OPC-PACs (1ml /kg body weight) intraperitoneally twice a week until the end of the experiment. OPC-PACs treated MNU-induced mammary gland carcinogenesis yielded a significant decrease in the size of tumors per animal compared to the untreated MNU-induced group. Cytotoxicity examination revealed that there are substantial decreases in the activities of ALT and AST (sensitive indicators of liver damage) in the OPC-PACs treated MNU-induced tumor group compared to the untreated MNU-induced tumor group as shown in **(Figure 7B)**. Furthermore, the decrease of OPC-PACs treated group was significantly higher than the control group. OPC-PACs treatment significantly decreased ($P \leq 0.001$) creatinine (a sensitive indicator of kidney damage) in the treated group compared to the untreated MNU-induced group; on the contrary, OPC-PACs treatment showed no effect the tested in sera for total protein *versus* other untreated and control groups as shown in **(Figure 7B)**.

4. Discussion

Maintaining a healthy diet and lifestyle is essential in preventing several types of cancer (35). Most natural products are extracted from plants and have the potential to be promising anti-cancer agents(36). Blocking multiple cancer-associated signaling pathways is pivotal to inhibiting cancer cell proliferation and progression. Several plants' natural products, such as oligomeric OPC-PACs extracted from grape seeds, impede tumor proliferation by inhibiting several cancer-associated pathways without cellular toxicity.

In the present study, we investigated the anticancer mechanistic effect of OPC-PACs extracts using two human cancer cell lines as the following: human hepatocellular carcinoma (HepG2) and human breast carcinoma (Zr-75-1). In addition, we focused on the possibility of using OPC-PACs extract to target multiple oncogenic crosstalk of several pathways that impart tumor pathogenicity. For that sake, cellular viability, proliferation, oncogenic signaling expression, and apoptosis induction were determined after 48h of treatment with several concentrations of OPC-PACs extracts. Our data revealed that OPC-PACs treatment for 48h inhibited cell proliferation and induced apoptosis associated with significant cell morphological changes, histone release from fragmented DNA, and increased caspase-3 activation in a dose-dependent manner. In tested cancer cells, treated cells by OPC-PACs validated the modulation of some oncogenic signals such as p-ERK, STAT3, β-catenin, and apoptotic signal of Bax.

It is known that apoptosis protects against cancer progression by eliminating the hyperproliferating and mutated cancer cells (37). Several studies have proved that OPC-PACs can prevent the proliferation of cancer cells in different cancer types by blocking their cell cycle. The antiproliferative effects of OPC-PACs have been demonstrated in liver cancer cell lines and murine hepatoma (Hepa1c1c7) cells (38). According to our findings, OPC-PACs have shown anti-cancer and inhibitory properties

on cell viability and the ability to reduce proliferative oncogenic signaling pathways and induce apoptosis in both HepG2 and Zr-75-1. The early stage of apoptosis is associated with several morphological alterations, such as cell shrinkage and DNA fragmentation, chromatin condensation, and formation of apoptotic bodies in both HepG2 and Zr-75-1 cells treated with (¼ IC_{50}, ½ $IC_{50,}$ and IC_{50}) OPC-PACs for 48 h. (39). Moreover, the cell growth and clonal formation assays showed that OPC-PACs inhibit the tested cell lines' proliferation and cloning formation ability.

The data of WST-1 proved the cytotoxic effects of OPC-PACs on HepG2 and Zr-75-1 cells after treatment with different concentrations of OPC-PACs (0 ~120 mg/ml) for 48 h, suggesting that OPC-PACs are effective in inhibiting HepG2 and Zr-75-1 cells viability and proliferation. It was reported on the IC_{50} values of OPC-PACs on three cancer cell lines that showed significant induction of cell cytotoxicity in a concentration and time-dependent manner. The published data of human prostatic adenocarcinoma (PC-3), human colorectal adenocarcinoma (HT-29), and human breast carcinoma (MCF-7) cell lines showed that different concentration OPC-PACs extracts inhibited cell viability and proliferation detected by cell cytotoxicity after 24 and 48 h. (40).

The selection of drug combinations depends on the cancer cells' genetic nature and signaling pathways. Testing OPC-PACs' effect on oncogenic crosstalk signaling pathways in cancer and if it has limited clinical applications due to toxicities. Our data introduced OPC-PACs extracts as a potent inhibitor for the cellular oncogenic proliferation signals of the tested liver and breast cancer cell lines with various biological characteristics without any detected cellular toxicity. These observations revealed the promise of OPC-PACs extracts as a therapeutic candidate against liver and breast cancer cells and the possibility of using it as a clinical therapeutic.

It has been reported that cancer growth, apoptosis, and metastasis are linked to MAPK/ERK pathway-related proteins(41). ERK is essential in cellular proliferation, migration, and invasion, and JNK and p38 MAPK are responsible for cell apoptosis(42). The activation of the RAF/MAPK/ERK signaling pathway in HCC was found to be associated with the advanced stage of the disease(43). Therefore, we investigated the potential anticancer effect of OPC-PACs on the MAPK/ERK pathway by examining the protein expression of T-ERK1/2 against p-ERK1/2 by western blot analysis. The phosphorylation is essential for ERK1/2 activation, so the evaluation of the phosphorylated ERK1/2 and its relation to the total protein abundance provides an indication and proof of the potential effect of extracted OPC-PACs on ERK1/2 activity. After 48 hours of treatment with OPC-PACs, the levels of p-ERK1/2 significantly decreased in HepG2 and Zr-75-1 cells. However, there were no notable changes in the total abundance of ERK1/2. The potential of our study on OPC-PACs and their role in curing resistant and malignant tumors shed light on the molecular mechanism of the extracted OPC-PACs. Several studies reported that OPC-PACs stimulate apoptotic pathways by producing reactive oxygen species(44,45). Others have indicated that the process of apoptosis is integrated with the overexpression of pro-survival genes, like some of the BCL-2 family members, and pro-apoptotic genes, like Bax, that have a

central role in the regulation of the apoptotic process. Bax overexpression triggers the cells to enter the apoptosis stage, causing increased caspase-3 (40). The present study led to a possible mechanistic part of extracted OPC-PACs on apoptosis induction linked to a significant increase of nuclear apoptosis, caspase-3 increased activities, and Bax up-regulation linked to the substantial inhibition of the oncogenic signal's crosstalk.

Late stages of tumor progression have been detected with the accumulation of nuclear β-catenin. Aggressive tumor growth is associated with the presence of mutated β-catenin, which regulates the expression of many target genes mediating cellular processes such as proliferation and migration (46). β-catenin is phosphorylated by GSK-3β and casein kinase 1 α (CK1α) causing its ubiquitination and followed by subsequent degradation(18). The next step will be the nuclear accumulation of β-catenin and the downstream target genes, which are subsequently activated, including genes responsible for cell proliferation such as PCNA, cyclins and cyclin-dependent kinases, and genes responsible for tumor progression such as matrix metalloproteinases (18). Our data showed that treatment of both HepG2 and Zr-75-1 cancer cell lines with OPC-PACs for 48 h inhibited the expression of β-catenin through degradation of the β-catenin, causing nuclear reduction and cytosolic accumulation, suggesting that extracted OPC-PACs have an inhibitory effect against both HepG2 and Zr-75-1 cell lines.

STAT−3 pathway is essential in several cellular processes, including tumorigenesis, cell cycle machinery, proliferation, and apoptosis. Uncontrolled gene regulation is associated with unchecked STAT−3 activation in cancer; aberrant activation of STAT−3 is involved in several cancer types by modulating p53 synthesis and inhibiting its protective effect on stability gene expression (47). Furthermore, STAT−3 inhibits and tolerates the damage and stress of cancer cells, suggesting that constant activation of STAT−3 involves cellular differentiation, proliferation, and invasion (48). Our data are consistent with previously published data revealing that extracted OPC-PACs inhibited STAT-3 signaling pathways and prevented cellular proliferation and progression by induction of apoptosis in both tested cell lines. It was reported that OPC-PACs inhibited the expression of the JAK2/p-STAT3 axis, which in turn inhibited the initiation and progression of the A549 lung cancer cell line, suggesting the possible anti-cancer effects of OPC-PACs in lung cancer effect through inhibiting STAT3 signaling pathway (49).

Additionally, two pathways play a role in STAT-3 inactivation the RAS/MAPK pathway and the non-receptor tyrosine kinase pathway. RAS and its downstream signaling of MAPK, a serine/threonine protein kinase, modulate differentiation, proliferation, and cell pathology. Several reports revealed the possible role of RAS-regulated MAPK in STAT-3-induced autophagy and tumorigenesis (50,51), and the effect of STAT-3 on gene regulation is significantly decreased by inhibiting MAPK expression through phosphorylation of tyrosine residues (52). Several other studies identified the regulatory role of the RAS/ERK axis by crosstalk with the Wnt/β-catenin pathway, which is connected directly with the cell's proliferation and transformation(53,54) through activation of Wnt3a to the Raf-1-

MEK-ERK axis, revealing direct interaction of the two pathways. The regulatory effect of Wnt/β-catenin signaling on the MEK-ERK pathway in the proliferation and transformation of cells was further approved by modulating the Wnt/β-catenin axis components, such as GSK3β, Axin, and APC (54,55). Wnt/β-catenin controls the stability regulation of RAS through GSK3β kinase that mediated phosphorylation of RAS, suggesting the established crosstalk between the Wnt/β-catenin and RAS-ERK pathways (56). The tumorigenesis of many several cancers is initiated and promoted through an abnormal irregular stimulation of the Wnt/β-catenin and RAS-ERK pathways; therefore, targeting the inhibition of both β-catenin and RAS-ERK pathways is an effective mechanism that sheds light on the development of anticancer drugs (57).

Blocking multiple pathways may be an effective strategy in targeting cancer cells by targeting several oncogenic signaling resulting in undesired off-target mediators. Our data showed no toxicity in mice's tested cell lines upon oral administration for three weeks. However, further investigations are needed to determine pharmacodynamic data availability to understand its effects on human health.

In conclusion, we introduce OPC-PAC extract from grape seeds as a natural, non-toxic, safe compound with anticancer properties against liver and breast cancer cell lines by inhibiting cellular viability, proliferation, and vital crosstalk among cellular pathways as seen in the (**Figure 8**). In addition, OPC-PACs induced nuclear apoptosis upregulated Bax expression and increased caspase enzyme activity by inhibiting the oncogenic signaling pathways of β-catenin, STAT-3, and p-ERK. *In vivo*, OPC-PACs significantly decreased MNU-induced mammary tumor volumes. The present study sheds light on the anticancer activities of OPC-PACs which in turn introduce OPC-PACs as an upcoming phytochemical with no significant cytotoxicity for cancer treatment. The significance of data is related to the current great attention on using naturally occurring compounds with anticancer activities, such as extracted OPC-PACs, which might be a potential source of molecular target-based cancer prevention and acquired resistance in cancer patients undergoing targeted therapies.

Ethical Approval and Consent to participate: The manuscript does not contain clinical studies or patient data. The authors declare no competing interests.

Human Ethics: Not applicable

Consent for publication: All authors reviewed and approved the manuscript.

Availability of supporting data: The datasets generated during and/or analyzed during the current study are available from the corresponding author upon reasonable request.

Competing interests: There is no conflict of interest.

Funding: Self-funding

Acknowledgment

Not applicable.

References

1. Ferlay J, Colombet M, Soerjomataram I, Parkin DM, Piñeros M, Znaor A, et al. Cancer statistics for the year 2020: An

overview. Int J Cancer. 2021 Aug 15;149(4):778–89.

2. Ravishankar D, Rajora AK, Greco F, Osborn HelenMI. Flavonoids as prospective compounds for anti-cancer therapy. Int J Biochem Cell Biol. 2013 Dec;45(12):2821–31.
3. Ky I, le Floch A, Zeng L, Pechamat L, Jourdes M, Teissedre PL. Tannins. In: Encyclopedia of Food and Health. Elsevier; 2016. p. 247–55.
4. de la Iglesia R, Milagro FI, Campión J, Boqué N, Martínez JA. Healthy properties of proanthocyanidins. BioFactors. 2010 Mar 15;36(3):159–68.
5. Rasmussen SE, Frederiksen H, Struntze Krogholm K, Poulsen L. Dietary proanthocyanidins: Occurrence, dietary intake, bioavailability, and protection against cardiovascular disease. Mol Nutr Food Res [Internet]. 2005 Feb 1;49(2):159–74. Available from: https://doi.org/10.1002/mnfr.200400082
6. Gu L, Kelm MA, Hammerstone JF, Beecher G, Holden J, Haytowitz D, et al. Concentrations of Proanthocyanidins in Common Foods and Estimations of Normal Consumption. Journal of Nutrition. 2004;134(3).
7. Ravindranathan P, Pasham D, Balaji U, Cardenas J, Gu J, Toden S, et al. Mechanistic insights into anticancer properties of oligomeric proanthocyanidins from grape seeds in colorectal cancer. Carcinogenesis. 2018;39(6).
8. Lei C, Tang X, Li H, Chen H, Yu S. Molecular hybridization of grape seed extract: Synthesis, structural characterization and anti-proliferative activity in vitro. Food Research International. 2020;131.
9. Xu H, Zhao X, Liu X, Xu P, Zhang K, Lin X. Antitumor effects of traditional Chinese medicine targeting the cellular apoptotic pathway. Drug Des Devel Ther. 2015;9.
10. Chojnacka K, Lewandowska U. The Antiangiogenic Activity of Polyphenol-Rich Extracts and Its Implication on Cancer Chemoprevention. Vol. 36, Food Reviews International. 2020.
11. Meeran SM. Proanthocyanidins inhibit mitogenic and survival-signaling in vitro and tumor growth in vivo. Frontiers in Bioscience. 2008;13(13):887.
12. 11. Toden S, Ravindranathan P, Gu J, Cardenas J, Yuchang M, Goel A. Oligomeric proanthocyanidins (OPCs) target cancer stem-like cells and suppress tumor organoid formation in colorectal cancer. Sci Rep. 2018;8(1).
13. Ran L, Yang C, Xu M, Yi Z, Ren D, Yi L. Enhanced aqueous two-phase extraction of proanthocyanidins from grape seeds by using ionic liquids as adjuvants. Sep Purif Technol. 2019 Nov;226:154–61.
14. Torres-Acosta MA, Mayolo-Deloisa K, González-Valdez J, Rito-Palomares M. Aqueous Two-Phase Systems at Large Scale: Challenges and Opportunities. Biotechnol J. 2019 Jan;14(1):1800117.
15. Kim NY, Jang MK, Lee DG, Yu KH, Jang H, Kim M, et al. Comparison of methods for proanthocyanidin extraction from pine (Pinus densiflora) needles and biological activities of the extracts. Nutr Res Pract. 2010;4(1):16.
16. Xu X, Zhang M, Xu F, Jiang S. Wnt signaling in breast cancer: biological mechanisms, challenges and opportunities. Mol Cancer. 2020 Dec 24;19(1):165.
17. Lecarpentier Y, Claes V, Vallée A, Hébert J. Thermodynamics in cancers: opposing interactions

between PPAR gamma and the canonical WNT/beta-catenin pathway. Clin Transl Med. 2017 Dec 12;6(1).
18. VAID M, SINGH T, PRASAD R, KATIYAR SK. Bioactive proanthocyanidins inhibit growth and induce apoptosis in human melanoma cells by decreasing the accumulation of β-catenin. Int J Oncol. 2016 Feb;48(2):624–34.
19. Guo Y, Pan W, Liu S, Shen Z, Xu Y, Hu L. ERK/MAPK signalling pathway and tumorigenesis (Review). Exp Ther Med. 2020 Jan 15;
20. Peng W xin, Huang J guo, Yang L, Gong A hua, Mo YY. Linc-RoR promotes MAPK/ERK signaling and confers estrogen-independent growth of breast cancer. Mol Cancer. 2017 Dec 17;16(1):161.
21. Wang L, Zhan J, Huang W. Grape Seed Proanthocyanidins Induce Apoptosis and Cell Cycle Arrest of HepG2 Cells Accompanied by Induction of the MAPK Pathway and NAG-1. Antioxidants. 2020 Nov 28;9(12):1200.
22. Huynh H, Nguyen TTT, Chow KHKP, Tan PH, Soo KC, Tran E. Over-expression of the mitogen-activated protein kinase (MAPK) kinase (MEK)-MAPK in hepatocellular carcinoma: Its role in tumor progression and apoptosis. BMC Gastroenterol. 2003 Dec 8;3(1):19.
23. Yu H, Pardoll D, Jove R. STATs in cancer inflammation and immunity: a leading role for STAT3. Nat Rev Cancer. 2009 Nov;9(11):798–809.
24. Sultan A, Xie J, LeBaron M, Ealley E, Nevalainen M, Rui H. Sultan AS, Xie J, LeBaron MJ, Ealley EL, Nevalainen MT, Rui H.. Stat5 promotes homotypic adhesion and inhibits invasive characteristics of human breast cancer cells. Oncogene 24: 746-760. Oncogene. 2005 Feb 1;24:746–60.
25. Pérez-Ortiz JM, Alguacil LF, Salas E, Hermosín-Gutiérrez I, Gómez-Alonso S, González-Martín C. Antiproliferative and cytotoxic effects of grape pomace and grape seed extracts on colorectal cancer cell lines. Food Sci Nutr [Internet]. 2019 Aug 2;7(9):2948–57. Available from: https://pubmed.ncbi.nlm.nih.gov/31572588
26. Behari J, Zeng G, Otruba W, Thompson MD, Muller P, Micsenyi A, et al. R-Etodolac decreases β-catenin levels along with survival and proliferation of hepatoma cells. J Hepatol. 2007 May;46(5):849–57.
27. Hames BD. Gel Electrophoresis of Proteins: A Practical Approach (3rd ed.). In Oxford: Oxford University Press; 1998.
28. Bolt MW, Mahoney PA. High-Efficiency Blotting of Proteins of Diverse Sizes Following Sodium Dodecyl Sulfate–Polyacrylamide Gel Electrophoresis. Anal Biochem. 1997 May 1;247(2):185–92.
29. Huang XJ, Choi YK, Im HS, Yarimaga O, Yoon E, Kim HS. Aspartate Aminotransferase (AST/GOT) and Alanine Aminotransferase (ALT/GPT) Detection Techniques. Sensors. 2006 Jul 31;6(7):756–82.
30. Doumas BT, Bayse DD, Carter RJ, Peters T, Schaffer R. A candidate reference method for determination of total protein in serum. I. Development and validation. Clin Chem. 1981 Oct 1;27(10):1642–50.
31. Gowda S, Desai PB, Kulkarni SS, Hull V V, Math AAK, Vernekar SN. Markers of renal function tests. N Am J Med Sci [Internet]. 2010 Apr;2(4):170–3. Available from:

https://pubmed.ncbi.nlm.nih.gov/22624135
32. Jacobson MD, Weil M, Raff MC. Programmed Cell Death in Animal Development. Cell. 1997 Feb;88(3):347–54.
33. Datta R, Kojima H, Yoshida K, Kufe D. Caspase-3-mediated Cleavage of Protein Kinase C θ in Induction of Apoptosis. Journal of Biological Chemistry. 1997 Aug;272(33):20317–20.
34. Liu X, Zou H, Slaughter C, Wang X. DFF, a Heterodimeric Protein That Functions Downstream of Caspase-3 to Trigger DNA Fragmentation during Apoptosis. Cell. 1997 Apr;89(2):175–84.
35. Anand P, Kunnumakara AB, Sundaram C, Harikumar KB, Tharakan ST, Lai OS, et al. Cancer is a Preventable Disease that Requires Major Lifestyle Changes. Pharm Res [Internet]. 2008;25(9):2097–116. Available from: https://doi.org/10.1007/s11095-008-9661-9
36. Choi H, Cho SY, Pak HJ, Kim Y, Choi J yun, Lee YJ, et al. NPCARE: database of natural products and fractional extracts for cancer regulation. J Cheminform [Internet]. 2017;9(1):2. Available from: https://doi.org/10.1186/s13321-016-0188-5
37. Leone A, Longo C, Gerardi C, Trosko JE. Pro-Apoptotic Effect of Grape Seed Extract on MCF-7 Involves Transient Increase of Gap Junction Intercellular Communication and Cx43 Up-Regulation: A Mechanism of Chemoprevention. Int J Mol Sci. 2019 Jul 2;20(13):3244.
38. Carnésecchi S, Schneider Y, Lazarus SA, Coehlo D, Gossé F, Raul F. Flavanols and procyanidins of cocoa and chocolate inhibit growth and polyamine biosynthesis of human colonic cancer cells. Cancer Lett. 2002 Jan;175(2):147–55.
39. Bottone MG, Santin G, Aredia F, Bernocchi G, Pellicciari C, Scovassi AI. Morphological features of organelles during apoptosis: an overview. Cell. 2013;2:294–305.
40. Albogami S. Proanthocyanidins reduce cellular function in the most globally diagnosed cancers in vitro. PeerJ. 2020 Sep 15;8:e9910.
41. Kim EK, Choi EJ. Pathological roles of MAPK signaling pathways in human diseases. Biochimica et Biophysica Acta (BBA) - Molecular Basis of Disease. 2010 Apr;1802(4):396–405.
42. Boutros T, Chevet E, Metrakos P. Mitogen-Activated Protein (MAP) Kinase/MAP Kinase Phosphatase Regulation: Roles in Cell Growth, Death, and Cancer. Pharmacol Rev. 2008 Sep;60(3):261–310.
43. Huynh H, Nguyen TTT, Chow KHKP, Tan PH, Soo KC, Tran E. Over-expression of the mitogen-activated protein kinase (MAPK) kinase (MEK)-MAPK in hepatocellular carcinoma: Its role in tumor progression and apoptosis. BMC Gastroenterol. 2003 Dec 8;3(1):19.
44. Yun S, Chu D, He X, Zhang W, Feng C. Protective effects of grape seed proanthocyanidins against iron overload-induced renal oxidative damage in rats. Journal of Trace Elements in Medicine and Biology. 2020;57.
45. Xu J-P. Natural substances for cancer prevention. 1st Edition. Boca Raton: CRC Press; 2018.
46. Liu J, Xiao Q, Xiao J, Niu C, Li Y, Zhang X, et al. Wnt/β-catenin signalling: function, biological mechanisms, and therapeutic

opportunities. Signal Transduct Target Ther. 2022 Jan 3;7(1):3.
47. Niu G, Wright KL, Ma Y, Wright GM, Huang M, Irby R, et al. Role of Stat3 in Regulating p53 Expression and Function. Mol Cell Biol. 2005 Sep 1;25(17):7432–40.
48. Gu Y, Mohammad I, Liu Z. Overview of the STAT-3 signaling pathway in cancer and the development of specific inhibitors (Review). Oncol Lett. 2020 Feb 13;
49. Wu Y, Liu C, Niu Y, Xia J, Fan L, Wu Y, et al. Procyanidins mediates antineoplastic effects against non-small cell lung cancer via the JAK2/STAT3 pathway. Transl Cancer Res. 2021 May;10(5):2023–35.
50. Lakshmanachetty S, Balaiya V, High WA, Koster MI. Loss of TP63 Promotes the Metastasis of Head and Neck Squamous Cell Carcinoma by Activating MAPK and STAT3 Signaling. Molecular Cancer Research. 2019 Jun 1;17(6):1279–93.
51. Liang F, Ren C, Wang J, Wang S, Yang L, Han X, et al. The crosstalk between STAT3 and p53/RAS signaling controls cancer cell metastasis and cisplatin resistance via the Slug/MAPK/PI3K/AKT-mediated regulation of EMT and autophagy. Oncogenesis. 2019 Oct 9;8(10):59.
52. Yan K, Xu X, Wu T, Li J, Cao G, Li Y, et al. Knockdown of PYCR1 inhibits proliferation, drug resistance and EMT in colorectal cancer cells by regulating STAT3-Mediated p38 MAPK and NF-κB signalling pathway. Biochem Biophys Res Commun. 2019 Dec;520(2):486–91.
53. Park KS, Jeon SH, Kim SE, Bahk YY, Holmen SL, Williams BO, et al. APC inhibits ERK pathway activation and cellular proliferation induced by RAS. J Cell Sci. 2006 Mar 1;119(5):819–27.
54. Kim SE, Choi KY. EGF receptor is involved in WNT3a-mediated proliferation and motility of NIH3T3 cells via ERK pathway activation. Cell Signal. 2007 Jul;19(7):1554–64.
55. Kim SE, Yoon JY, Jeong WJ, Jeon SH, Park Y, Yoon JB, et al. H-Ras is degraded by Wnt/β-catenin signaling via β-TrCP-mediated polyubiquitylation. J Cell Sci. 2009 Mar 15;122(6):842–8.
56. Jeong WJ, Yoon J, Park JC, Lee SH, Lee SH, Kaduwal S, et al. Ras Stabilization Through Aberrant Activation of Wnt/β-Catenin Signaling Promotes Intestinal Tumorigenesis. Sci Signal. 2012 Apr 10;5(219).
57. Jeong WJ, Ro EJ, Choi KY. Interaction between Wnt/β-catenin and RAS-ERK pathways and an anti-cancer strategy via degradations of β-catenin and RAS by targeting the Wnt/β-catenin pathway. NPJ Precis Oncol. 2018 Feb 20;2(1):5.

Fig. 1

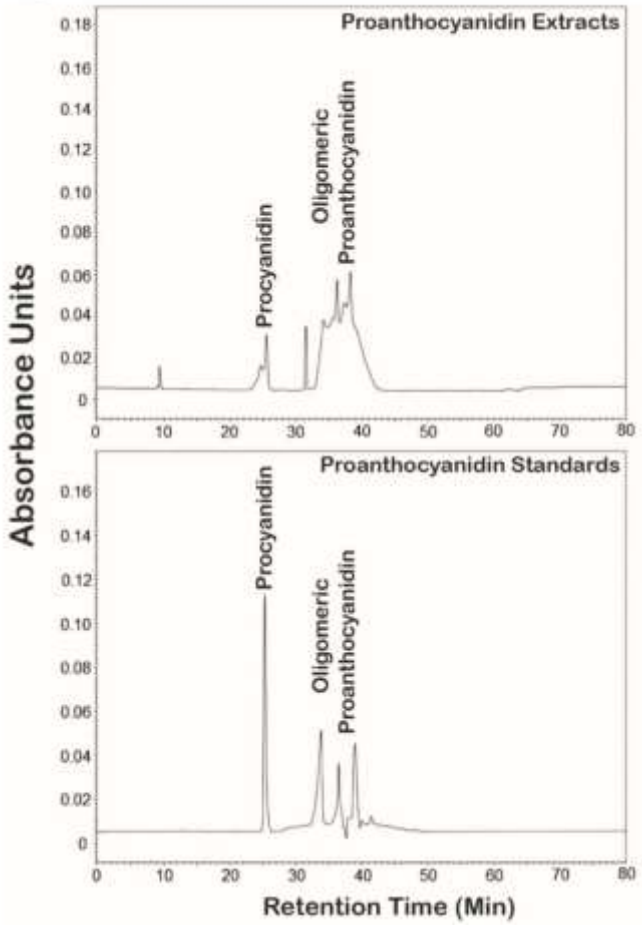

Fig. 1: HPLC chromatogram of the fraction of grape seed oligomeric-PACs. The upper panel showed the chromatogram of procyanidin B2, the oligomeric grape seed PACs standard, and the lower panel offered PACs and proanthocyanidins standards.

Fig. 2A

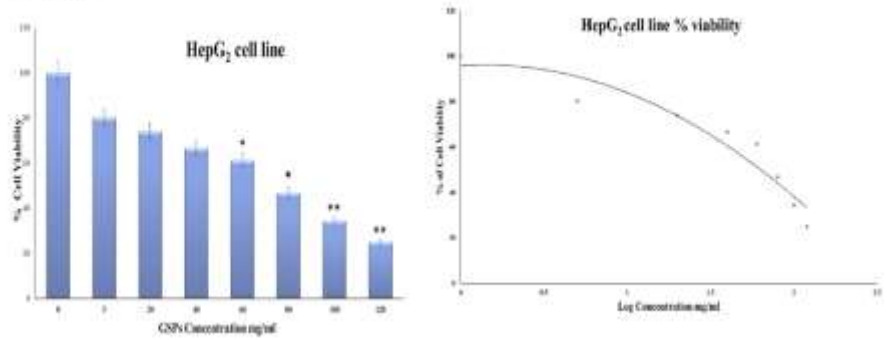

Fig. 2B

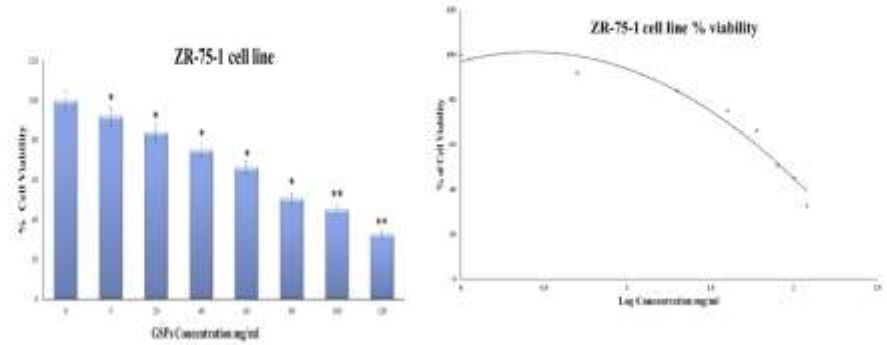

Fig. 2A and B: The left panel showed the inhibitory effect of oligomeric-PACs on the viability of HepG2 and Zr-75-1 cell lines, respectively. Cells were grown in a complete DMEM medium and treated with different concentrations (0 ~ 120 mg/ml) oligomeric-PACs for 48 h, and cells' viability was determined by WST-1 assay. Cell viability (%) was compared to control (untreated)—the correct panel Dose–response curve of oligomeric-PACs of HepG2 and Zr-75-1 cell lines. The calculated IC_{50} of oligomeric-PACs for HepG2 and Zr-75-1 cells was (63.1 ±0.024 mg/ml) and (61.6 ± 0.016 mg/ml), respectively. Each data point averages three independent experiments and is expressed as ± MSD. P-value *P < 0.05 and < 0.01 compared to untreated control cells.

Fig. 3A

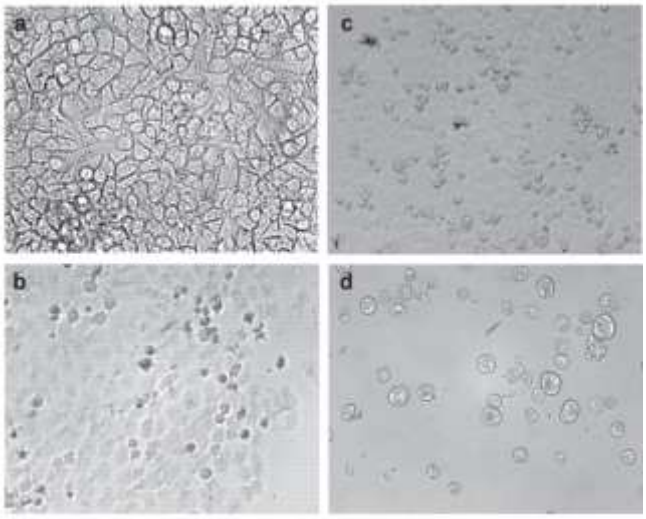

HepG2 cell line

Fig. 3B

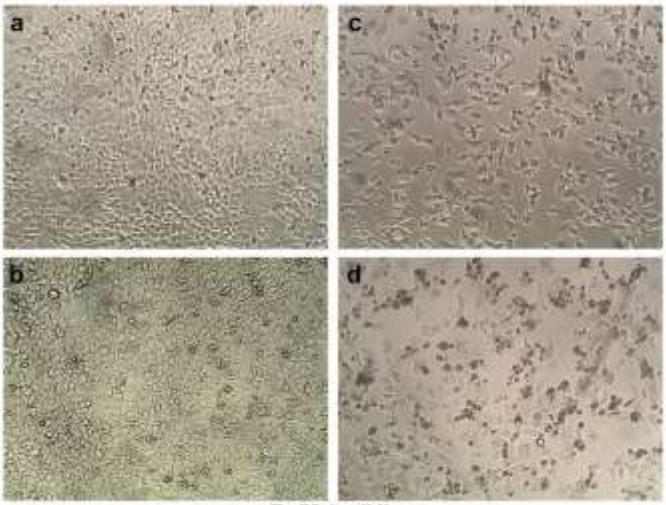

Zr-75-1 cell line

Fig. 3A and B: Oligomeric-PACs treatment induced morphological changes of HepG2 and Zr-75-1 cell lines. Cells were treated with or without oligomeric-PACs for 48 has the following: (a) Control, (b) ¼ IC50 Oligomeric-PACs, (c) ½ IC50 Oligomeric-PACs, (d) IC50 Oligomeric-PACs. Cells were investigated under the inverted microscope at 400X magnification. The above data are representative of three independent experiments.

Fig. 4A

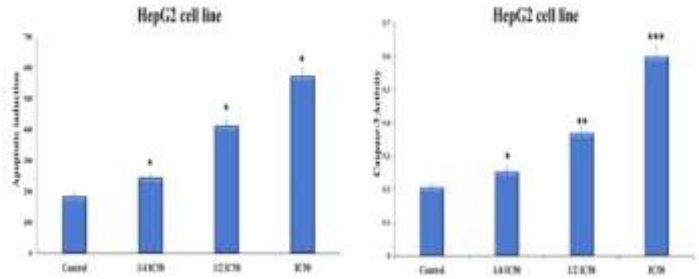

Fig. 4B

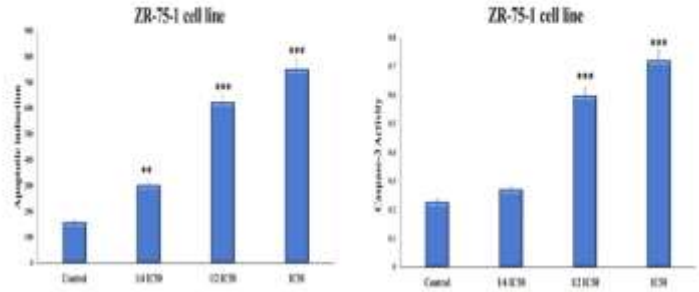

Fig. 4A and B: Oligomeric-PACs induced apoptosis and caspase-3 activation induction in HepG2 and Zr-75-1 cell lines—the left panel: Oligomeric-PACs induced histone-release and apoptotic induction in HepG2 and Zr-75-1 cells. Cells were treated with oligomeric-PACs for 48 h, and histone-release activity was determined using a specific ELISA assay kit according to the manufacturer's protocol—the right panel: Caspases-3 activity in HepG2 and Zr-75-1 cell lines. Cells were treated with oligomeric-PACs for 48 h, and caspase-3 enzymatic activity was determined using a specific colorimetric assay kit according to the manufacturer's protocol, as explained under the Materials and Methods section. Each point averages three independent experiments and is expressed as $M \pm SD$. P-value was calculated versus control cells: $*P < 0.05$, $**P < 0.01$, and $***P < 0.001$.

Fig. 5A

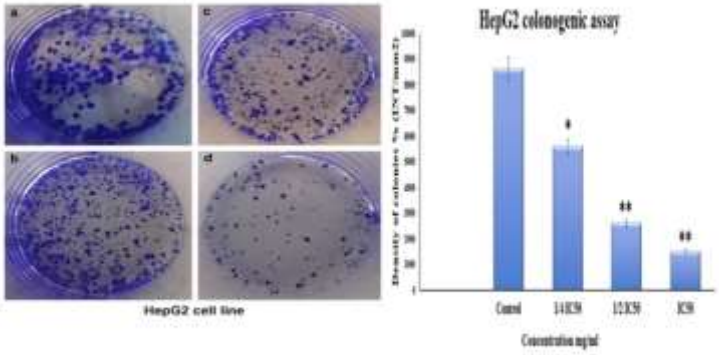

Fig. 5B

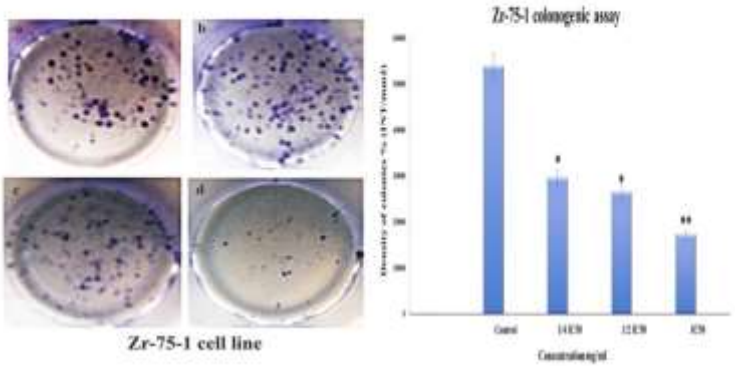

Fig. 5A and B: Oligomeric-PACs inhibited clonogenicity of HepG2 and Zr-75-1 cells. Cells were investigated before and after treatment with different oligomeric-PACs concentrations for 48 h. The left panel: The colony formation assay in HepG2 and Zr-75-1 cells. The right panel: The relative density of colony formation capacity in HepG2 and Zr-75-1 cells was quantified by Quantity One software. (a) Control, (b) ¼IC_{50}, (c) ½$IC_{50,}$ and (d) IC_{50}. Each point averages three independent experiments and is expressed as M ± SD. P-value was calculated versus control cells: *P < 0.05 and **P < 0.01.

Fig. 6A

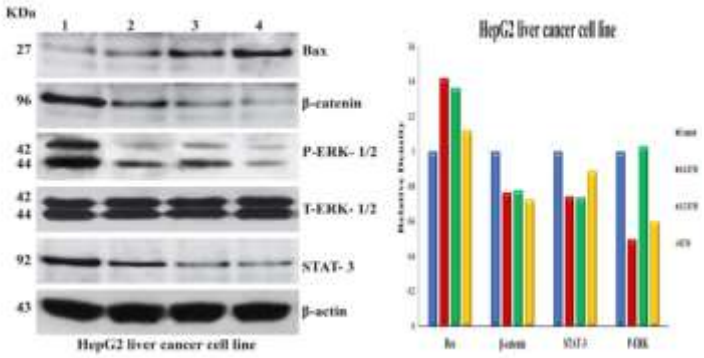

Fig. 6B

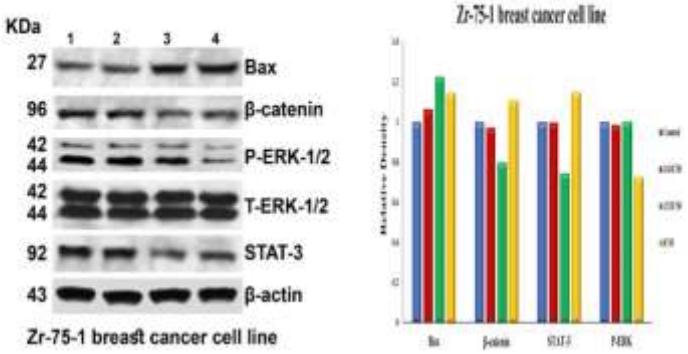

Fig. 6A and B: Using western blot analysis, oligomeric-PACs inhibited signaling crosstalk in HepG2 and Zr-75-1 cells. The left panel: Protein expression levels of Bax, β-catenin, ERK, pERK1/2, and STAT-3 were detected by western blot analysis. The right panel: Relative density of the tested protein expression in HepG2 and Zr-75-1 cells was quantified by Quantity One software. The cell lysate was subjected to 10% SDS-PAGE. Proteins were transferred to the nitrocellulose membrane and probed with the indicated antibodies, as explained in the Materials and Methods section. Anti-β-actin was used as a loading control. Protein expressions were quantified and normalized to β-actin and controls.

Fig. 7A

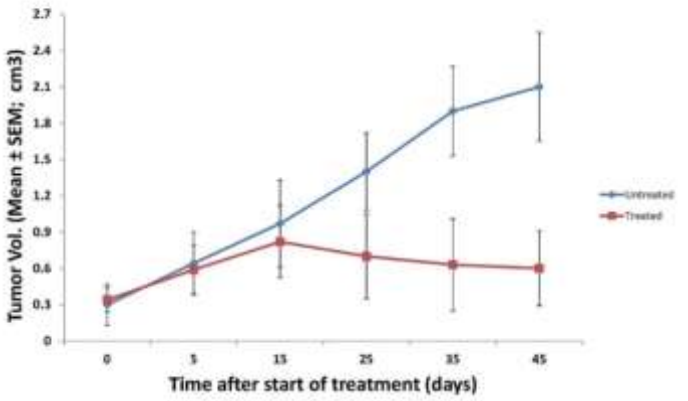

Fig. 7B

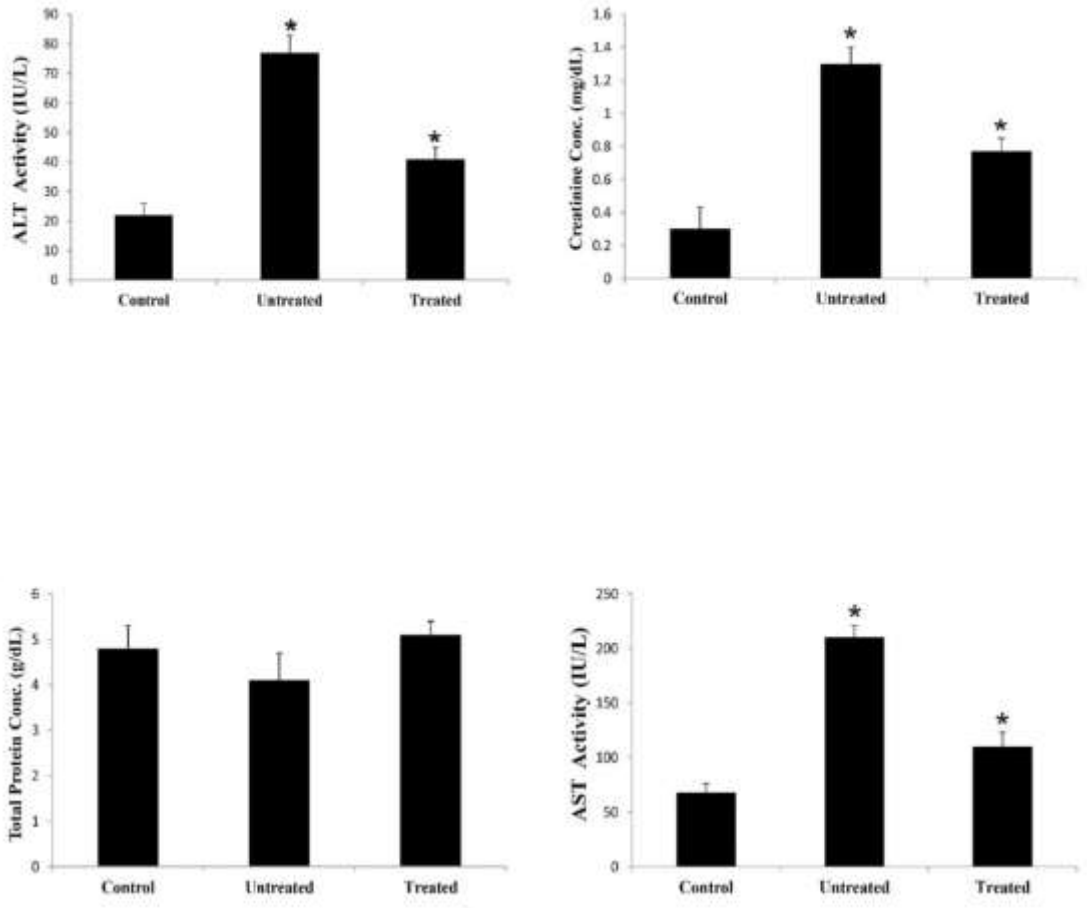

Fig. 7A and B: Biochemical tests and cytotoxicity of Oligomeric-PACs, *in vivo*. Wister Albino mice were divided into three groups of 10 mice, each following groups as described under the Materials and Methods section: Mock-healthy controls without MNU-induction, induced untreated-MNU was given intraperitoneally (30 mg/kg), and induced treated-MNU plus LD_{50} OPC-PACs. OPC-PACs were injected intraperitoneally (1ml/kg body weight); all control animals received an injection of the solvent, saline. Mice were treated three times a week for 45 days**. Fig. 7A** showed that OPC-PACs treatment significantly decreased the MNU-induced breast tumor volumes compared to the untreated MNU-induced group. For the cytotoxicity examination, the sera of tested groups were analyzed spectrophotometrically for liver and kidney functions, including the activities of AST and ALT, creatinine, and total protein, as shown in **Fig. 7B**. Statistically, significance was detected by calculating P-value versus control cells; *P-value < 0.05; **P < 0.01 and ***P < 0.001 were considered statistically significant.

Fig. 8

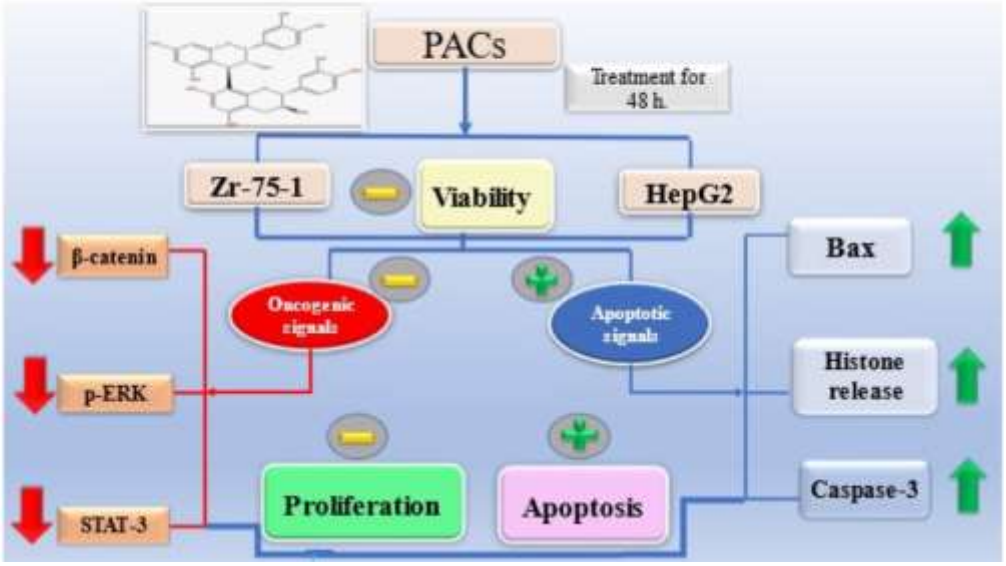

Fig. 8: The proposed mechanism of action of Oligomeric-PACs as an anticancer compound.